Available online at www.sciencedirect.com
SCIENCE DIRECT®
Sensors and Actuators B 103 (2004) 290–299
SENSORS AND ACTUATORS B CHEMICAL
www.elsevier.com/locate/snb

Optical fiber probes for fluorescence based oxygen sensing

P.A.S. Jorge [a,b,*], P. Caldas [a,b,c], C.C. Rosa [a,b], A.G. Oliva [d], J.L. Santos [a,b]

[a] *Unidade de Optoelectrónica e Sistemas Electrónicos, INESC Porto, Rua do Campo Alegre, 687. Porto 4169 007, Portugal*
[b] *Departamento de Física da Faculdade de Ciências da Universidade do Porto, Rua do Campo Alegre, 687. Porto 4169 007, Portugal*
[c] *Escola Superior de Tecnologia e Gestão—Instituto Politécnico de Viana do Castelo, Av. do Atlântico, Apartado 574, Viana do Castelo 4901-908, Portugal*
[d] *Instituto de Tecnologia Química e Biológica (ITQB), Universidade Nova de Lisboa, Apartado 127, Oeiras 2781-901, Portugal*

Available online 4 June 2004

Abstract

An optical fiber sensing system, for monitoring oxygen aiming in vivo nuclear magnetic resonance (NMR) applications is presented. Oxygen detection is based on the dynamic quenching of the fluorescence of a ruthenium complex trapped in the porous structure of a sol–gel silica film. Oxygen concentration is determined by phase-modulation fluorometry. Preliminary results concerning the characterization of doped sol–gel thin films deposited by dip coating in glass slides and in optical fiber probes are presented. Four different probe configurations are tested and compared. Best results are obtained with a fiber taper configuration which shows reproducibility and best excitation efficiency. This structure is fully characterized and some considerations regarding optimal fiber optical sensing probes for O_2 detection are addressed.

Keywords: Optical fiber; Oxygen sensor; Phase fluorometry

1. Introduction

The remote monitoring of oxygen in many biomedical and environmental applications is of major importance. Fluorescence spectroscopy is a powerful technique for this purpose and a great research effort is being made in order to use it in the context of optical fiber sensors [1,2]. Optical fiber oxygen sensors are more attractive than conventional electrochemical devices because they have a fast response, do not consume oxygen and are immune to electromagnetic interference.

One of the situations where oxygen monitoring is crucial is in in vivo nuclear magnetic resonance (NMR). This is a very attractive technique to investigate cell metabolism due to its non-invasive characteristic. In NMR measurements, the quantity of oxygen available to the cell trough the probe is one of the most important parameters to monitor during an in vivo testing, since cellular metabolism varies as a function of the oxygen concentration of the medium. At present, the measurement of dissolved oxygen (DO) level is performed externally to the NMR probe by conventional procedures, namely perfusion and oxygen electrode. The strong electromagnetic field surrounding the NMR equipment avoids the use of oxygen electrodes in the measuring probe. The perfusion system used for transport of the cell media outside the probe, towards the oxygen electrode, induces errors due to changes in the sample environment (tubing transport, temperature). Therefore the development of an optoelectronic sensor prototype for the measurement of dissolved oxygen will be a very useful tool for metabolism studies of cell growth in in vivo NMR.

The present work reports some developments in the context of fiber optic based oxygen detection, which are important steps towards an integrated sensing system for utilization in harsh electromagnetic environments, as is the case of NMR application.

A popular method for optical oxygen detection is based on the dynamic quenching of the luminescence of ruthenium complexes [3]. The presence of oxygen quenches both the intensity, I, and the excited state lifetime, τ, of the fluorescent complex. Oxygen concentration is related to these parameters by the Stern–Volmer (SV) equation:

$$\frac{I_0}{I} = \frac{\tau_0}{\tau} = 1 + K_{SV}[O_2] \quad (1)$$

where I_0 and τ_0 are, respectively, the intensity and the lifetime in the absence of quencher, K_{SV} the SV constant and $[O_2]$ the concentration of oxygen. Direct measurement of either the intensity or the lifetime has problems associated.

* Corresponding author.
E-mail address: pjorge@inescporto.pt (P.A.S. Jorge).
URL: http://www.opto.inescn.pt.

0925-4005/$ – see front matter © 2004 Elsevier B.V. All rights reserved.
doi:10.1016/j.snb.2004.04.086

Intensity measurements demand the implementation of reference schemes in order to compensate for optical power drift due to optical source instability, coupling efficiency fluctuations and possible leaching and photo bleaching of the fluorophore. Direct lifetime measurements demand for high-speed electronics and fast pulsed optical sources. All these problems can be avoided using a phase-modulation technique [4,5].

Applying a sinusoidal modulation to the optical source results in a phase delay, ϕ, in the fluorescent emission that can be related to the lifetime by the equation:

$$\tan[\phi] = 2\pi f\tau \quad (2)$$

where f is the modulation frequency, which can be tuned, according to the luminescence lifetime, for optimum sensor sensitivity [6]. Using Eqs. (1) and (2) the phase delay information can easily be related with oxygen concentration. With this technique, low cost high brightness optical sources, like blue LEDs, which are suitable for excitation of many important fluorophores, can be used in association with standard photodetection.

One of the main problems associated with the development of commercially viable optical chemical sensors regards the immobilization of the fluorophores in the tip of optical fiber probes in an easy, cheap and reproducible way. However, a great research effort is being made towards the application of the sol–gel process in the context of optical chemical sensors applications in general and oxygen sensors in particular. The sol–gel process is very well adapted for thin film fabrication, at ambient temperature, and the process parameters can be controlled in order to produce a thin micro-porous matrix in which the fluorophore is entrapped and accessible to analyte molecules [7,8].

Another critical issue in sensor optimization regards the sensing head configuration, namely its efficiency in exciting the sensing film and capturing the resulting fluorescence signal carrying the measurement information [9]. Four different sensing probe configurations were tested using the same basic set-up, based on phase-modulation fluorometry. In all the studied geometries, the sensing ruthenium complex immobilization was carried out by entrapment in a porous silica matrix produced by the sol gel process and deposited in the sensing probes by dip coating. In the context of sensor optimization, different methods of coupling the excitation radiation into the fiber system were also experimented. All sensing geometries are compared and full characterization of the configuration with best performance is presented.

2. Experimental

All the sensing geometries were tested using the same basic phase fluorometry set-up represented in the scheme of Fig. 1. A high brightness blue LED (470 nm-Nichia) was used as excitation source. The radiation was guided into one of the arms of a multimode silica glass optical fiber coupler (coupling ratio of 50/50; core and cladding diameters of 550 and 600 μm, respectively). The LED emission was sinusoidally modulated at 75 kHz. This modulation frequency was determined by the system bandwidth limitations. The sensing probes were connected to one of the output arms of the fiber coupler by and adapted FC/PC connector; the other coupler output was immersed in index matching liquid in order to eliminate any blue light back reflection. The resulting fluorescence signal was long-pass filtered by two consecutive colored glass filters (OG550-Schot, $\lambda_{cutoff} = 550$ nm) before the detector. Detection was carried out by a high gain photodiode. A reference signal, from the LED modulation, and the detected fluorescence signal were fed into a lock-in amplifier (SRS 850). In these conditions the lock-in output was a phase signal proportional to the oxygen concentration. The sensing probes were placed in a small gas chamber connected to O_2 and N_2 supplies. A standard O_2 meter was used to monitor the oxygen level in the chamber.

In order to maximize the coupling of the LED radiation into the fiber system three different techniques were tested: a standard microscope objective system; a small diameter ball lens; and direct butt coupling of the fiber to an LED whose encapsulation was partially removed and polished.

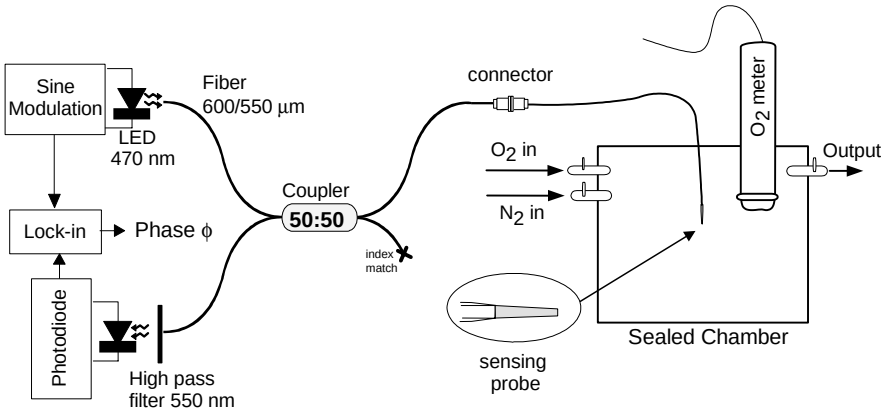

Fig. 1. Experimental set-up used to test the sensing probe configurations.

The sensing films were fabricated following standard sol–gel processing procedure: a precursor, tetraethoxysilane (TEOS), was mixed with a solvent (ethanol) in a volume ratio of 1 and with water (0.01 M HCL) in a molar ratio of 4. These steps provided a solution that would become a porous silica glass after drying. In order to obtain an oxygen sensitive thin film the solution was doped with a ruthenium complex. The sensing complex chosen to perform the experimental tests was Tris(2,2′-bipyridine) ruthenium(II) chloride hexahydrate [Ru(bpy)$_3$], because it is a well known and cost-effective oxygen sensor ($\lambda_{excitation} = 470$ nm; $\lambda_{emission} = 610$ nm) [10,11]. After stirring the base solution for 10 min, the ruthenium powder was added in a 0.01 M concentration. Further stirring was applied for 2 h. The solution was then left to age at ambient temperature. All films were produced by dip-coating (3 mm/s) both in the glass slides and in the optical fibers probes. Drying of the films was performed at 20 °C for 24 h.

Four sensing head geometries were fabricated and coated with a sensing film. The different configurations can be seen in Fig. 2. In all cases the optical fiber lead (550/600 μm) guided the excitation radiation to the sensing region and captured the emitted fluorescence signal, leading it back to detection. Configuration (a) is an extrinsic configuration, the sensing probe is a glass slide coated with the sensing thin film that is in contact with the polished fiber tip. Configurations (b)–(d) are intrinsic configurations where the sensing film is deposited in the fiber tip. In configuration (b) only the fiber tip is coated. In configuration (c) the cladding of a 2 cm length section at the fiber tip was previously removed with hydrofluoridric acid (HF); the tip and the uncladded side of the fiber were then coated with the sensing film. Finally, in configuration (d), the uncladded fiber tip (2 cm) was tapered, by dip coating in HF, into a conical shape (550 μm at the base, 300 μm at the top), and then coated with the sensing film.

In order to compare the devices sensitivity some parameters were evaluated. One of them is the quenching response defined by

$$Q = \frac{I_{N_2} - I_{O_2}}{I_{N_2}} \quad (3)$$

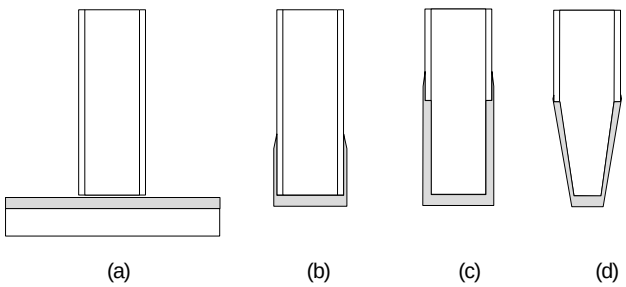

Fig. 2. Fiber probe geometries: (a) glass slide; (b) fiber tip; (c) uncladded tip; (d) taper.

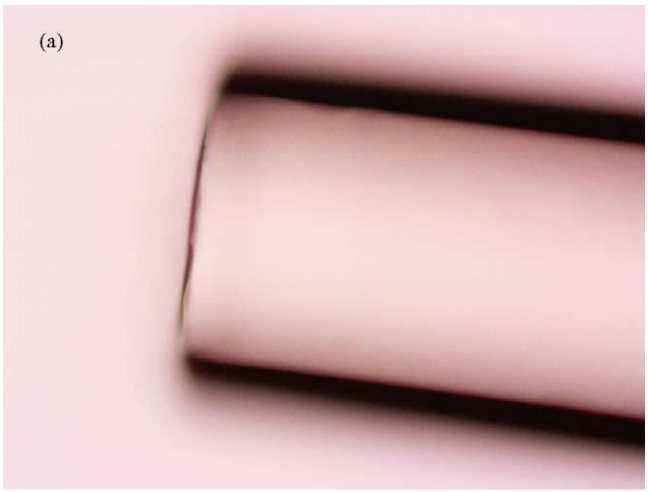

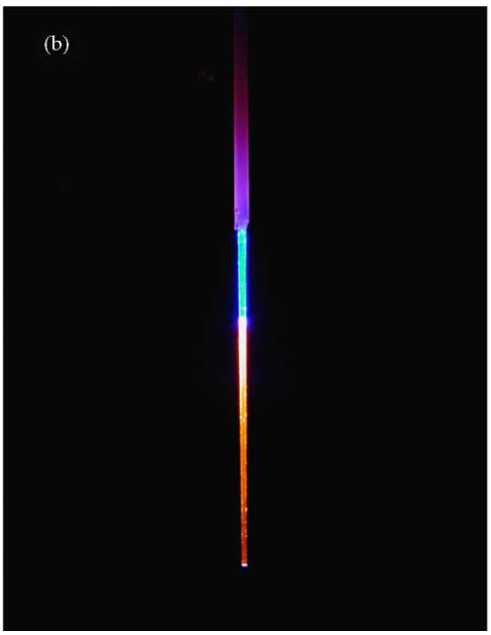

Fig. 3. (a) Microscope photograph of a fiber tip; (b) photograph of fiber taper in a 100% N_2 environment.

where I_{N_2} and I_{O_2} are the fluorescence intensities in N_2 and O_2 saturated atmospheres, respectively. To assess phase sensitivity independent of the modulation frequency, it was also evaluated the lifetime difference:

$$\Delta\tau = \tau_{N_2} - \tau_{O_2} \quad (4)$$

where τ_{N_2} and τ_{O_2} are the excited state lifetimes in saturated atmospheres of N_2 and O_2, respectively. Lifetime was

Table 1
Power coupling efficiencies with different techniques

Coupling system	Coupling efficiency (%)	Alignment
Microscope	2.6	Very sensitive
Ball lens	8.0	Sensitive
Butt coupling, 550 μm core	8.0	Straightforward
Butt coupling, 1 mm core	20.0	Straightforward

estimated by plotting tan[ϕ] (Eq. (2)) as a function of modulation frequency.

In the detection of the fluorescence signal care was taken in order to effectively eliminate any backscattered blue radiation. With this objective two consecutive long-pass colored glass filters were used. This provided attenuation by a factor of 10^6. This was done because even a small blue contribution to the detected signal can result in an appreciable error in the phase read by the lock-in. If the signal reaching the detector has a red fluorescence signal and a residual excitation (blue) contribution, the resulting detected sinusoidal signal will have a power amplitude P_d and a phase ϕ_d:

$$P_d \sin(\omega t + \phi_d) = P_b \sin(\omega t + \phi_b) + P_r \sin(\omega t + \phi_r) \quad (5)$$

where P_b and P_r are the blue and red power amplitudes, respectively, ϕ_b and ϕ_r their respective phases, and ω the angular modulation frequency. From well known trigonometric relations, it turns out that

$$P_d^2 = P_d^2 + P_r^2 + 2P_b P_r \cos(\phi_r - \phi_b) \quad (6)$$

and

$$\tan\phi_d = \frac{P_b \sin\phi_b + P_r \sin\phi_r}{P_b \cos\phi_b + P_r \cos\phi_r} \quad (7)$$

The oxygen measurement information is in signal ϕ_r. This way, due to the fact that the lock-in delivers ϕ_d instead of ϕ_r, a phase measurement error is committed. A similar error occurs with the amplitude measurement. The values of P_d, P_b, ϕ_d and ϕ_b corresponding to 100% of N_2 were measured experimentally in configurations (b)–(d). The phase ϕ_r was then numerically calculated with Eqs. (6) and (7), and the respective relative phase error was evaluated for each sensing head structure.

Table 2
Comparative results for the tested fiber probe configurations

Geometry	Q (%)	$\Delta\tau$ (ns)	Response time (s)	P_d (nW)	P_b (nW)
(a) Slide	30–40	72–176	9–11	0.36	–
(b) Tip	34–44	246	20–60	0.65	118
(c) Uncladded	55	250	20	0.72	19
(d) Taper	65	350	11–13	1.29	18

3. Results and discussion

The results regarding the different power coupling techniques can be observed in Table 1. Using a standard coupling method (collimating and focusing with 10× microscope objectives) only 2.6% of the radiation emitted by the LED was injected into the optical fiber. This poor result is mainly due to the LED high divergence angle (≈15°), causing high insertion losses. Also, this configuration turned out to be very sensitive to fiber alignment.

With a 10 mm diameter ball lens, an efficiency of approximately 8% was achieved. This increase results from the insertion loss of the collimating system being much smaller with a single glass sphere than with two separate microscope objectives. With this system fiber alignment was easier.

After polishing the LED encapsulation, the semiconductor emitting surface was only 100 μm away from the fiber tip and an efficiency of ≈8% was achieved. In this set-up fiber alignment was straightforward. After polishing, the LED divergence angle increased to 45°, but because of the proximity to the emitting area the power density reaching the fiber top was much higher. Considering that the LED emitting area (≈900 μm diameter) was bigger than the fiber core (≈550 μm diameter), better results are expectable for the

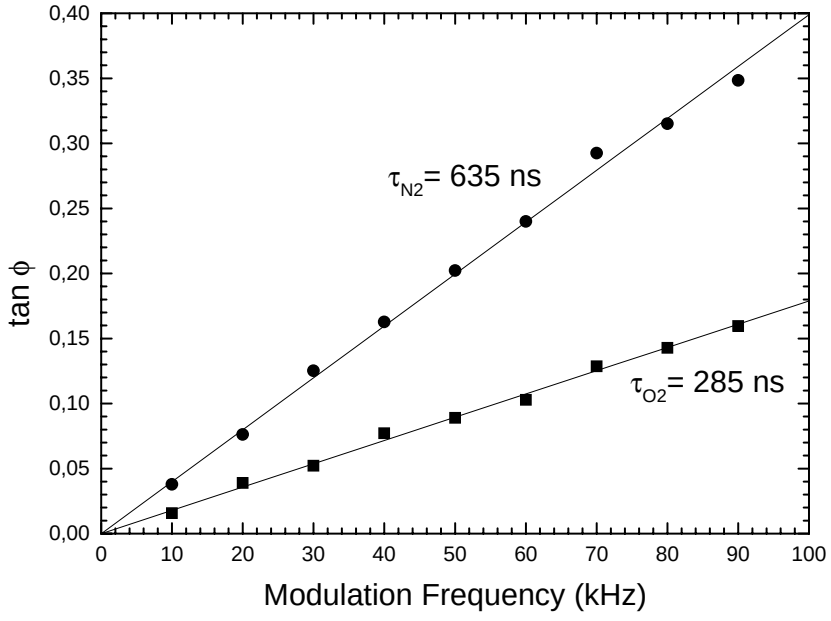

Fig. 4. Plot of tan ϕ as a function of modulation frequency for the fiber taper in 100% O_2 and 100% N_2.

case where larger fiber core diameters are used. Indeed for a fiber with a 1 mm core diameter light coupling efficiencies of ≈20% were achieved.

In the experimental set-up of Fig. 1 the butt-coupling configuration was used with a 550 μm core fiber. In such situation, an optical power of 70 μW was available in each output of the fiber coupler.

Preliminary tests, in gaseous environments, were performed using the coated glass slides in order to characterize the sol gel thin films. The parameters Q and $\Delta\tau$ were evaluated as a function of the solution aging time, from 2 h to more than 48 h at 20 °C. Both these parameters increased with increasing aging time. Values for Q parameter between 30 and 40% were obtained. Values for $\Delta\tau$ varied between 77 and 176 ns. As stated in the literature, this behavior results from increased film porosity and easier oxygen diffusion into the matrix [8]. This traduces in higher quenching efficiency and increased oxygen sensitivity. The unquenched lifetime, τ_0, decreased with increased aging time, 630 and 545 ns, for 2 and 24 h aging time, respectively. With a dip coating speed of 3 mm/s, film thickness between 600 and 800 nm were obtained (measured with a perfilometer). The response time of the sensing films when they undergone O_2/N_2 saturation cycles varied between 9 and 11 s (framed to the 10 and 90% reference levels). In the slide configuration the detected fluorescence emission was very weak ($P_d \approx 0.36$ nW), and due to a low signal to noise ratio (SNR) the phase signal was unstable. The resulting Stern–Volmer plots were non-linear indicating that the sensing complex had a heterogeneous distribution inside the porous silica

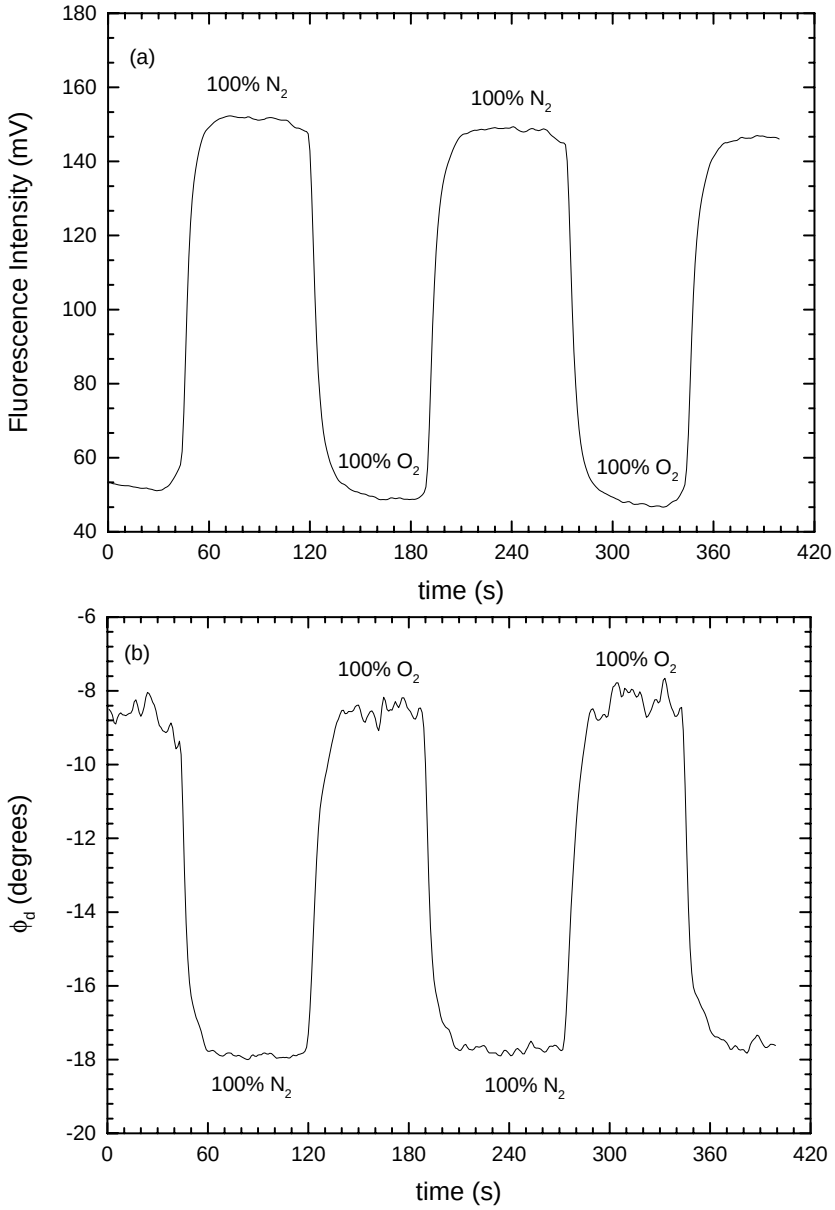

Fig. 5. Response of fiber taper to O_2/N_2 saturation cycles: (a) fluorescence intensity response; (b) phase response.

matrix. However, after a thermal treatment for 3 h at 80 °C, a great improvement in linearity ($R > 0.99$) was obtained at the expense of a slight decrease in the Q values.

In all fiber probes tested the coating speed was 3 mm/s and the solution aging time was more than 48 h. The main results obtained with all configurations are summarized in Table 2.

With configuration (b) no uniform thin films could be obtained because they were thicker in the tip than in the lateral surface, a consequence of the fabrication process. However, as can be seen in Fig. 3a, the film deposited smoothly in the fiber lateral surface and in the tip the film structure is also relatively flat. The response time of several fiber tips with this geometry, with the same sol–gel parameters, varied from 20 to 60 s. This shows that, with dip coating, it is not possible to obtain repeatable films, with uniform thickness, in the fiber tip. In spite of that, due to the increased thickness and a more efficient fluorescence coupling, a significant increase in SNR was observed. In comparison to configuration (a) the value of P_d increased by a factor of 1.8. Although the coating parameters were similar in all geometries, smaller values for Q and $\Delta\tau$ were obtained with this configuration. This can be related to film thickness and lower oxygen accessibility.

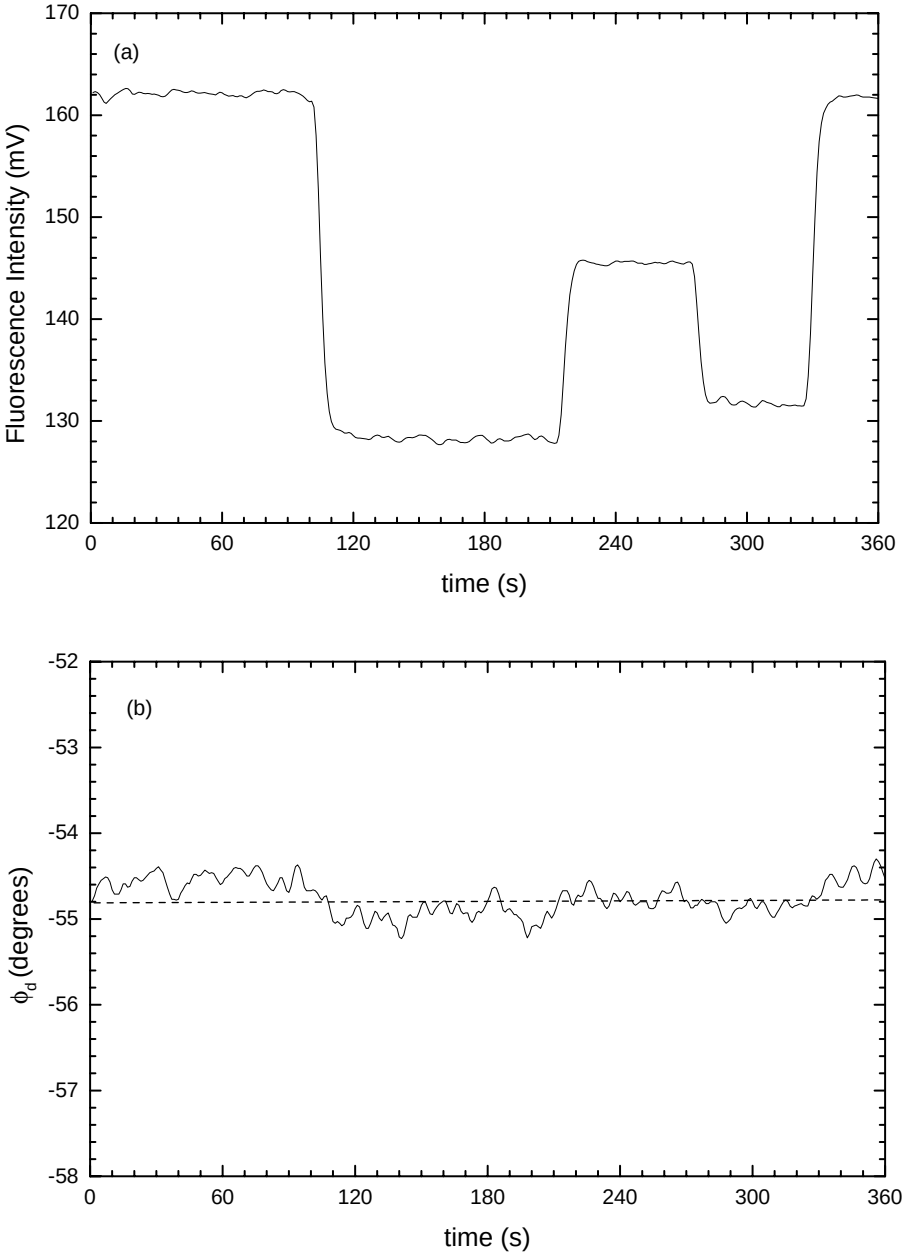

Fig. 6. Response of the sensor to variations in the optical power level injected into the fiber system, in an atmosphere of 21% O_2: (a) fluorescence intensity response; (b) phase response.

In configuration (c) uniform thin films were obtained in the uncladded side of the fiber. However, in the tip of the fiber the resulting films were non-uniform and too thick. Response times of approximately 20 s were obtained. This probably results from the averaging of a faster response from the side of the fiber with a much slower response from the top. Also some improvement in Q and $\Delta\tau$ parameters can be observed. However, no significant improvement in fluorescence coupling efficiency was observed in comparison to configuration (b). This may indicate that, in spite of the much bigger emission area, the contribution from the film in the fiber side to the fluorescence signal is small due to poor guiding from this region.

With configuration (d) due to the fiber geometry uniform thin films resulted both in the side and in the tip of the fiber. Shorter response times clearly indicate that the overall film thickness is similar to the ones obtained with the glass slides. This is also shown by the increase in Q and $\Delta\tau$, which also denote better quenching efficiency and sensitivity. With this configuration several sensing probes with very similar parameters were obtained showing good reproducibility. A great improvement in the SNR was registered in the tests performed with this configuration, being observed that P_d increased by a factor of 3.5 relatively to glass slides. Fig. 3b shows a photograph of the fluorescent taper in a 100% N_2 environment.

In the last column of Table 2 it can also be seen the degree of detected backscattered blue radiation in each configuration (P_b). Configuration (b) shows an increase, by a factor of 6, in the level of backscattered radiation when compared with configurations (c) and (d). Considering the respective levels of detected radiation (P_d) this means that, even after attenuation by a factor of 1000 (obtained with a single filter), a significant amount of blue light is mixed with the fluorescent signal. The attenuated blue power amplitude is still 18% of P_d in configuration (b), 2.6% of P_d in configuration (c) and 1.4% of P_d in configuration (d). According to numerical calculations using Eqs. (6) and (7) this will introduce phase errors of, respectively, 5.5, 0.7 and 0.4%. In the implemented experimental set-up this problem was avoided by using two cascaded long-pass filters corresponding to a 10^6 attenuation factor. In this case the error dropped below a negligible 0.005% in all configurations. In general double filtering is not a desirable situation from a practical point of view, but it can be bypassed by using of filters with higher performance. Anyway the desirable solution to this problem is to use sensing probe geometries which minimize the level of backscattered radiation. Also, if less blue radiation is being back reflected, this means, in principle, that a more efficient and uniform excitation is being accomplished in the sensing device.

By the results obtained it becomes clear that fiber tapering is a right step towards the sensing probe optimal configuration. This way, the full characterization of the sensing system was performed using a tapered sensing probe. In Fig. 4 it can be seen a plot of $\tan\phi$ as a function of modulation frequency f. It shows a great increase in the difference between phase measurements obtained in N_2 and O_2 saturated atmospheres as the modulation frequency increases from 10 to 90 kHz. In the present set-up a modulation frequency of 75 kHz was used due to bandwidth limitations of the overall system. For a luminescence lifetime of approximately 600 ns, the phase

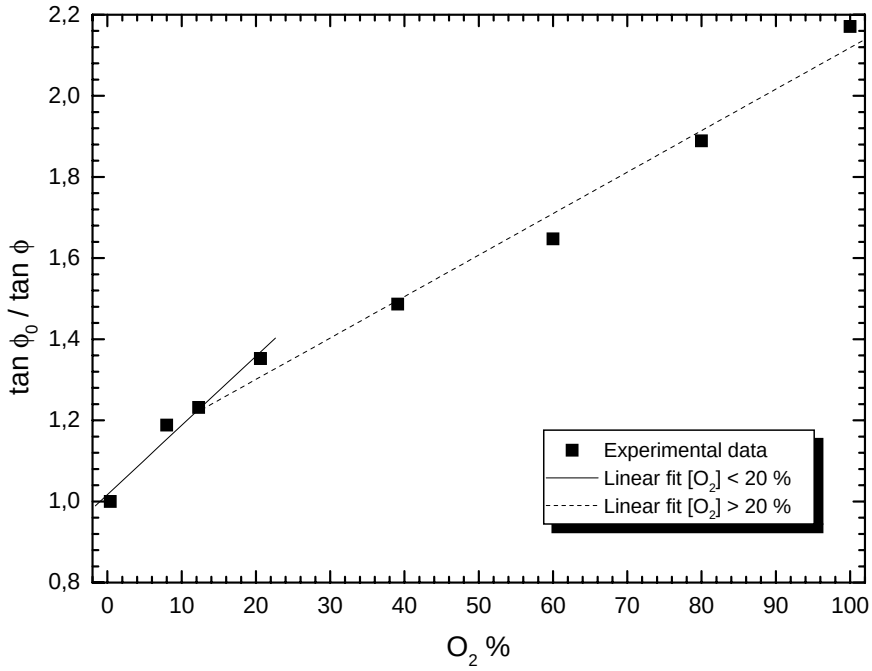

Fig. 7. Stern–Volmer plot obtained from the phase response of the fiber taper with a linear fit for the O_2 concentration range [0%; 20%] and other for the range [20%; 100%].

difference is expected to be maximum around 188 kHz, which is the ideal modulation frequency [5]. This way, an increase in modulation frequency is expected to improve sensor performance. In Fig. 5(a) and (b) the phase and the fluorescence intensity response of the sensing system to O_2/N_2 saturation cycles can be observed. The phase signal shows some instability indicating the need for SNR improvement. In order to demonstrate the phase insensitivity to optical power drift a simple test was performed. With the sensing head in a 21% O_2 atmosphere, the optical power injected into the fibre system was changed up to 25%. Fig. 6 shows the consequence of this variation in the intensity and phase of the fluorescence signal. Although a significant change in the intensity response occurs, the phase response remains essentially unchanged. This confirms the ability of the phase detection scheme to avoid power fluctuations induced errors.

The Stern–Volmer plots obtained from phase measurements with all configurations are clearly non-linear, indicating that the dopant is not homogeneously distributed within the silica matrix. Instead, the ruthenium complex occupies environments with different oxygen accessibilities. In this situation, the standard Stern–Volmer equation (Eq. (1)), based on a single exponential decay, no longer describes accurately the quenching behavior. Alternatively a dual exponential model, corresponding to two different dominant

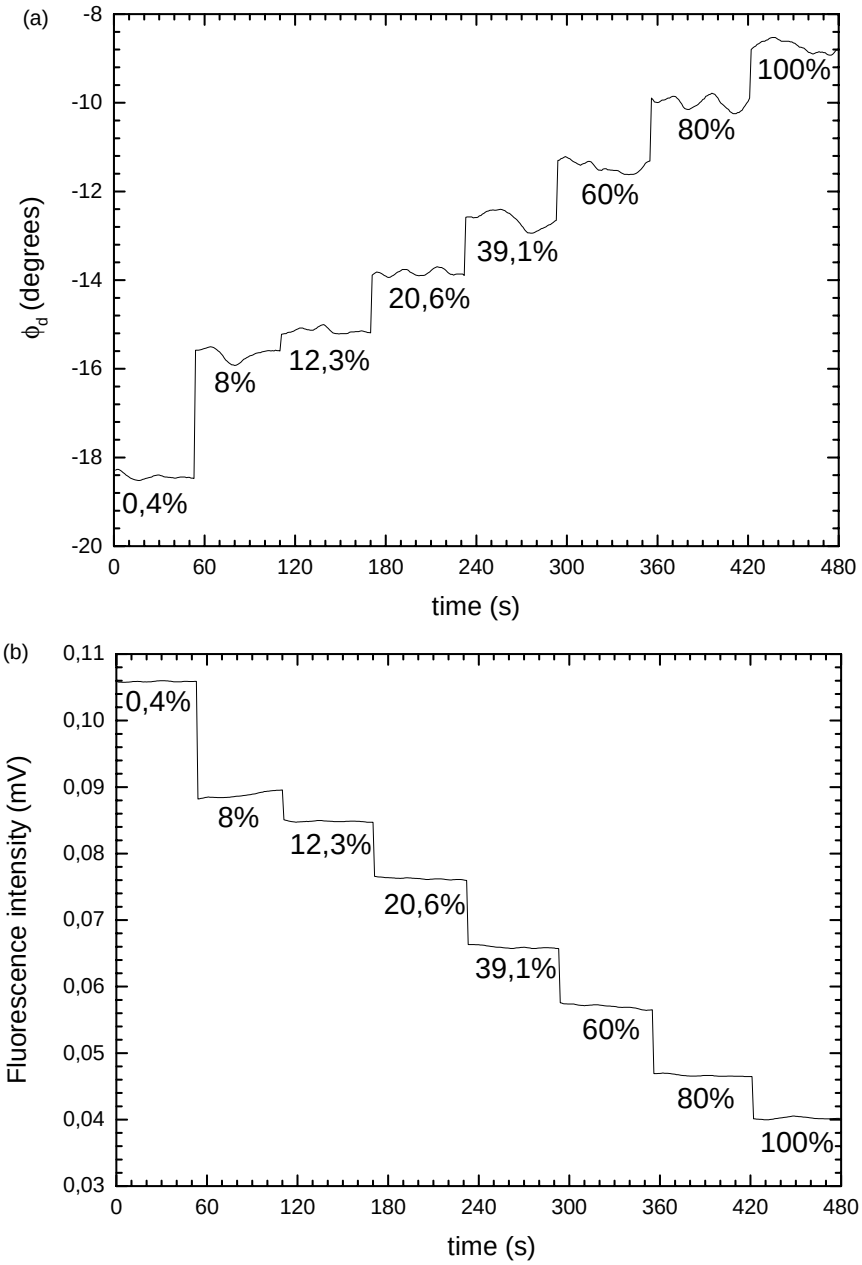

Fig. 8. System response to step variations of O_2 concentration level: (a) phase response; (b) fluorescence intensity response.

environments, is more adequate. In these cases a non-linear Stern–Volmer equation must be used [12]:

$$\frac{I_0}{I} = \left[\frac{f_1}{1 + K_{SV1}[O_2]} + \frac{f_2}{1 + K_{SV2}[O_2]}\right]^{-1} \quad (8)$$

In this expression f_1 and f_2 represent the fluorescence intensity contributions from each of the environments, and K_{SV1} and K_{SV2} the respective SV constants. This model was applied to the Stern–Volmer plot of the fiber taper. The following parameters where obtained: $f_1 = 0.917$, $f_2 = 0.083$, $K_{SV1} = 0.0092\%^{-1}$ and $K_{SV2} = 1.597\%^{-1}$. The fact that f_1 is much larger than f_2 indicates a clear predominance of one of the environments. The small heterogeneity existent is related with the sol gel film formation process. As it was observed with the glass slides, linearity can be improved with an adequate thermal treatment which promotes homogenization.

In order to estimate the sensor resolution, a simple approach was used. Fig. 7 shows a Stern–Volmer plot obtained with the fiber taper in which two O_2 concentration ranges with different sensitivities can be identified: higher sensitivity in the interval (0–20%); lower sensitivity in the interval (20–100%). Reasonably good linear fits can by adjusted to each one of these ranges. However for in vivo applications only the first interval is relevant. This way a linear fit ($R > 0.99$) was calculated to the first interval:

$$\frac{\tan\phi_0}{\tan\phi} = 1 + 0.01706[O_2] \quad (9)$$

In these conditions, Eq. (9) is an approximate transfer function of the sensing system and it was used to estimate system resolution. For this purpose the system phase response was recorded while steps of O_2 concentration where applied to the sensing probe. The results obtained can be observed in Fig. 8(a). The analysis of this data indicates a rms phase fluctuation of 0.06° in a system bandwidth of 78 mHz, which translates in a measurement phase resolution of $0.4^\circ/\sqrt{\text{Hz}}$. According to the system transfer function this corresponds to a minimum detectable oxygen variation of approximately 1%.

Similar analysis can be performed for the case of the fluorescence intensity response and the results are shown in Fig. 8(b). It is clear a more stable behavior when compared with the phase steps, which turns out in a better value for the minimum detectable oxygen concentration (0.1%) using the intensity detection method. This result is a consequence of the fact that the processing required to extract the phase information from the detected signal is more complex when compared with the one needed to recover the intensity and, therefore, more prone to error when the level of detected optical power is low. To obtain full advantage of the intrinsically favorable characteristics of the phase fluorometry technique, the optimization of the signal processing and of the power levels in the system is needed. In this context it is clear the importance of the sensing head design and of the efficient coupling of the excitation radiation into the fiber system, topics that were in the mainstream of the present work. Consequently, the focus was not the intrinsic properties of the sol–gel sensing films. Add to this the fact that TEOS based films are not suitable for liquid environments, typical of in vivo NMR applications, and were only used to test the performance of the sensing head configurations. For the purpose of DO measurements, hybrid precursors with substantially higher oxygen permeability should be used, which, in conjunction with the utilization of highly oxygen sensitive ruthenium complexes [13], will result in a high performance fiber optic sensing system in NMR applications.

4. Conclusion

A fiber optic sensing system aiming sensitive detection of dissolved oxygen in in vivo NMR applications was presented. With this objective the work focused on the conception, implementation and characterization of sol–gel based sensing fiber probes and on the optimization of the injection efficiency into the fiber system of the excitation radiation.

Four different fiber probes were tested in a fluorescence phase detection scheme. The tapered fiber tip structure showed the best performance, particularly in what concerns reproducibility, larger excitation efficiency and reduced level of backscattered excitation radiation. Higher radiation injection efficiency into the fiber system and relaxed alignment constrains were obtained with a butt-coupling geometry. The performance of the global sensing system in the determination of O_2 concentrations was assessed using both phase and intensity fluorometry. The results and indications acquired with this work, together with the utilization of tuned sol–gel sensing films, show the feasibility of a high performance fiber optic based sensing system for oxygen detection in in vivo NMR environments.

Acknowledgements

Pedro Jorge would like to acknowledge the financial support of Fundação para a Ciência e Tecnologia (FCT).

References

[1] B.D. MacCraith, et al., Fibre optic oxygen sensor based on fluorescence quenching of evanescent-wave excited ruthenium complexes in sol–gel derived porous coatings, Analyst 118 (1993) 385–388.
[2] M. Krihak, M.R. Shahriari, Highly sensitive, all solid state fibre optic oxygen sensor based on the sol–gel coating technique, Electron. Lett. 32 (1996) 240–241.
[3] A.K. McEvoy, C.M. McDonagh, B.D. MacCraith, Dissolved oxygen sensor based on fluorescence quenching of oxygen-sensitive ruthenium complexes immobilized in sol–gel-derived porous silica coatings, Analyst 121 (1996) 785–788.

[4] M.T. Murtagh, D.E. Ackley, M.R. Shahriari, Development of a highly sensitive fibre optic O_2/DO sensor based on a phase modulation technique, Electron. Lett. 32 (1996) 477–479.
[5] C. McDonagh, et al., Phase fluorometric dissolved oxygen sensor, Sens. Actuators B 74 (2001) 124–130.
[6] V.I. Ogurtsov, D.B. Papkovsky, Selection of modulation frequency of excitation for luminescence lifetime-based oxygen sensors, Sens. Actuators B 51 (1998) 377–381.
[7] C.M. McDonagh, B.D. MacCraith, A.K. McEvoy, Tailoring of sol–gel films for optical sensing of oxygen in gas and aqueous phase, Anal. Chem. 70 (1998) 45–50.
[8] C.M. McDonagh, et al., Characterisation of porosity and sensor response times of sol–gel-derived thin films for oxygen sensor applications, J. Non-Cryst. Solids 306 (2002) 138–148.
[9] L.C. Shriver-Lake, et al., The effect of tapering the optical fiber on evanescent wave measurements, Anal. Lett. 25 (1992) 1183–1199.
[10] P. Innocenzi, H. Kozuka, T. Yoko, Fluorescence properties of the $Ru(bpy)_3^{2+}$ complex incorporated in sol–gel-derived silica coating films, J. Phys. Chem. B 101 (1997) 2285–2291.
[11] K. Maruszweski, et al., Physicochemical properties of $Ru(bpy)_3^{2+}$ entrapped in silicate bulks and fiber thin films prepared by the sol–gel method, Chem. Phys. Lett. 314 (1999) 83–90.
[12] J.R. Lakowicz, Principles of Fluorescence Spectroscopy, Plenum Press, New York, 1999.
[13] A. Mills, Controlling the sensitivity of optical oxygen sensors, Sens. Actuators B 51 (1998) 60–68.

Biographies

P.A.S. Jorge graduated in Applied Physics (Optics and Lasers) from the University of Minho in 1996. He obtained his MSc degree in Lasers and Optoelectronics from the University of Porto in 2001. Currently he is a Researcher in the Optoelectronics and Electronic Systems Unit at INESC Porto working towards his PhD on optical fiber sensors based on fluorescence spectroscopy, by the Physics Department of University of Porto.

P. Caldas graduated in Applied Physics (Optics and Lasers) from the University of Minho in 1999. He received the MSc degree in Lasers and Optoelectronics at the Physics Department of University of Porto in 2003. Currently he is Researcher in the Optoelectronics and Electronic Systems Unit at INESC Porto and is teaching physics at Polythenic Institute of Viana do Castelo. He has been working in the area of optical fiber sensors and biosensors.

C.C. Rosa received her Technological Physics Engineering degree (1996) and Electrical Engineering and Computers Sciences MSc (1999) from Instituto Superior Técnico, Lisbon, Portugal. Presently at the Physics Department of the Sciences Faculty of Universidade do Porto, she is working in her PhD in the Optoelectronics Group of INESC Porto. Her research interest are on fibre based sensors with applications in bio-medical fields, in particular low-coherence interferometry techniques and biosensor development.

A.G. Oliva received his Agricultural Engineering degree from the University of Buenos Aires in 1984 and his PhD at the Hohenheim Universitaet, Stuttgart-Germany in 1989. He started in 1992 a biosensors laboratory in the Instituto de Tecnologia Química e Biológica, of the Universidade Nova de Lisboa/Portugal. His research interest and scientific activity include optical immunosensors and immunoassays for clinical diagnostics and bioprocess monitoring.

J.L. Santos graduated in Applied Physics (Optics and Electronics) by University of Porto (1983); PhD from the same university in 1993. Presently he holds the position of Associated Professor of the Physics Department of University of Porto, and he is in charge of the Optoelectronics and Electronic Systems Unit of INESC Porto. His research interests are connected to optical fibre technology, particularly fibre optic based sensors. He is Member of the Optical Society of America (OSA), International Society for Optical Engineering (SPIE) and the Planetary Society.